Lithospheric anisotropy structure inferred from collocated teleseismic and magnetotelluric observations: Great Slave Lake shear zone, northern Canada

David W. Eaton,[1] Alan G. Jones,[2,3] and Ian J. Ferguson[4]

Received 6 July 2004; revised 20 August 2004; accepted 15 September 2004; published 14 October 2004.

[1] Accurate interpretation of *SKS* shear-wave splitting observations requires inherently indeterminate depth information. Magnetotelluric electrical anisotropies are depth-constrained, and thereby offer possible resolution of the *SKS* conundrum. MT and teleseismic instruments, deployed across the Great Slave Lake shear zone, northern Canada, investigated lithospheric anisotropy and tested a hypothesis that seismic and electrical anisotropy obliquity can infer mantle strain shear-sense. Lithospheric mantle MT strike (N60°E) differs significantly from crustal MT strike (N30°E). *SKS* splitting vectors outside the shear zone exhibit single-layer anisotropy with fast axis parallel to upper-mantle MT strike and oblique to present-day plate motion (N135°W). Back-azimuth sensitivity at sites within the ~30 km wide shear-zone imply more complex layering, with two-layer inversion yielding an upper layer of ~N20°E and a lower layer of ~N66°E. The MT data help to constrain the depth location of *SKS* anisotropy and, taken together, support a model of fossil lithospheric anisotropy. *INDEX TERMS:* 7205 Seismology: Continental crust (1242); 7218 Seismology: Lithosphere and upper mantle; 8110 Tectonophysics: Continental tectonics—general (0905). **Citation:** Eaton, D. W., A. G. Jones, and I. J. Ferguson (2004), Lithospheric anisotropy structure inferred from collocated teleseismic and magnetotelluric observations: Great Slave Lake shear zone, northern Canada, *Geophys. Res. Lett.*, *31*, L19614, doi:10.1029/2004GL020939.

1. Introduction

[2] Birefringence analysis of *SKS* and other core-refracted shear waves is a widely used method to investigate seismic anisotropy of the mantle and, by inference, strain patterns associated with past and present-day mantle flow [*Silver*, 1996; *Savage*, 1999]. Upper-mantle seismic anisotropy is dominantly controlled by strain-induced lattice-preferred orientation of olivine crystals [*Savage*, 1999]. *S*-wave splitting is characterized by a time difference δt between perpendicularly polarized fast and slow arrivals, and a polarization direction ϕ_S of the fast shear wave. Significant *S*-wave splitting is common in most tectonic regimes, but upper-mantle anisotropy appears to be particularly well developed within 100 km of large-scale transcurrent plate boundaries [*Savage*, 1999].

[3] Similarly, magnetotelluric (MT) methods are used to determine electrical anisotropy and (or) 2-D structure of the mantle. The measurements are represented by geoelectric strike direction (ϕ_{MT}), the direction of maximum conductivity, and the phase difference ($\delta\theta$) between this and its orthogonal direction. Electrical anisotropy of the upper mantle has been attributed to preferred interconnection of a highly conducting mineral phase such as graphite [*Jones*, 1992; *Mareschal et al.*, 1995], or enhanced electrical conductivity caused by hydrogen diffusion along olivine *a*-axes [*Bahr and Simpson*, 2002]. In contrast to *S*-wave splitting, the depth-location of anisotropy is directly constrained by the frequency dependence of the MT response.

[4] Joint analysis of seismic and electrical anisotropy has the potential to provide useful constraints for interpreting mantle deformation. In a collocated MT-SKS study across the Grenville Front in eastern North America, *Ji et al.* [1996] noted a conspicuous and systematic obliquity of ~23° between ϕ_S and ϕ_{MT}. Based on petrofabrics in mantle xenoliths, they attributed this obliquity to differing directions of lattice-preferred orientation (seismic anisotropy) and shape-preferred orientation (electrical anisotropy) of mantle minerals. They correlated the geophysical fabrics to Archean transcurrent shear zones, located several hundred km north of their observation points.

[5] To test the obliquity hypothesis in a more definitive tectonic setting, we collected teleseismic and MT data across the Great Slave Lake shear zone (GSLsz), northern Canada; initial results are reported separately by *Eaton and Hope* [2003] and *Wu et al.* [2002], respectively. The *ca*. 1.9 Ga GSLsz is a transcurrent fault that accommodated up to 700 km of right-lateral displacement [*Ross*, 2002], in a tectonic setting analogous to modern strike-slip fault systems of southeast Asia [*Hoffman*, 1987]. It is exposed northeast of our study area within a 25-km wide mylonite corridor, where subvertical, deformation textures suggest non-coaxial flow [*Hanmer et al.*, 1992], in a manner similar to asymmetric petrofabrics described by *Ji et al.* [1996]. The exhumation of deep crustal levels of the GSLsz provides an opportunity to interpret *SKS* and MT observations above a major transcurrent fault, for which most of the brittle upper crust has been removed.

[6] The seismic and MT profiles straddle the GSLsz (Figure 1), locally buried beneath a thin (300–600 m) veneer of Paleozoic sedimentary rocks. A deep boundary in electrical conductivity [*Wu et al.*, 2002] and apparent offset of the Moho [*Eaton and Hope*, 2003] imply that the surface expression of the GSLsz is not significantly dis-

[1]Department of Earth Sciences, University of Western Ontario, London, Ontario, Canada.
[2]Geological Survey of Canada, Ottawa, Ontario, Canada.
[3]Now at School for Cosmic Physics, Dublin Institute for Advanced Studies, Dublin, Ireland.
[4]Department of Geological Sciences, University of Manitoba, Winnipeg, Manitoba, Canada.

0094-8276/04/2004GL020939$05.00

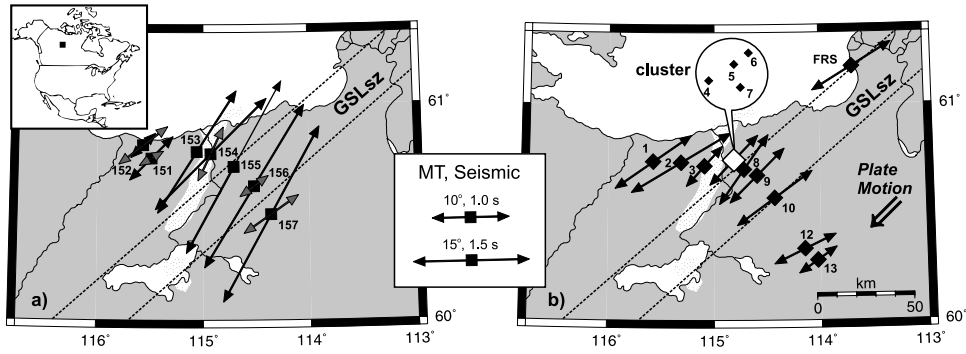

Figure 1. Locations of (a) the MT experiment [*Wu et al.*, 2002] and (b) the teleseismic experiment [*Eaton and Hope*, 2003] across the Great Slave Lake shear zone (GSLsz). Black and gray vectors (a) represent geoelectric strike vectors for 0.1–20 s (crustal) and 20–1000 s (lithospheric mantle) period bands, respectively. *S*-wave fast-axis directions (b) are single-layer averages. Stippled regions show local magnetic anomaly.

placed from its upper mantle root. Magnetic anomaly patterns indicate that the slightly younger and roughly parallel McDonald fault occurs well north of the profile [*Eaton and Hope*, 2003]. For both experiments the station interval was small (<15 km) to provide adequate spatial sampling of the uppermost mantle. This paper presents new analyses of both the teleseismic and MT data, including a two-layer inversion of the *SKS* observations and the first detailed joint interpretation of these datasets.

2. Geophysical Data

[7] A description of the MT data acquisition and processing is given by *Wu et al.* [2002]. Geoelectric-strike data (Figure 1a; see also auxiliary data[1]) were derived in three period bands, using the approach of *McNeice and Jones* [2001] with an assumed error floor of 2° in phase. Sensitivity to strike direction is indicated by the phase difference between the two orthogonal directions, and how well the model of distortion fits the data is indicated by the root mean chi-squared (RMS) misfit. Periods of ~20–50 s correspond to penetration to the base of the crust (40 km), and ~500–2,000 s to the base of the lithosphere (~200 km). MT strikes in the 10 Hz–20 s band are therefore representative of the middle and lower crust, 20–1,000 s of the bulk of the lithospheric mantle, and >1,000 s of the deepest lithosphere and into the asthenosphere. For the set of all 7 MT sites used, the best-fitting multi-site, multi-frequency regional strike direction at crustal penetrating periods is N36°E, and for lithospheric mantle periods is N60°E, roughly parallel to the regional strike of the shear zone. For periods sensitive to the deepest lithosphere and asthenosphere, the average strike is N70°E but with considerably greater scatter. For the 5 most-consistent stations, namely 151, 152, 155, 156 and 157, these three directions are N32°E, N58°E and N69°E.

[8] A description of the teleseismic data acquisition is given by *Eaton and Hope* [2003]. The particle-motion method of *Silver and Chan* [1991] was used with core-refracted phases *SKS* and *SKKS*. Bandpass filtered waveforms with transverse-component signal-to-noise ratio <2 were rejected, leaving 9 events for further analysis; tables listing the time and location of seismic events and individual splitting measurements are included as auxiliary material. To enhance reliability, we used the multi-event averaging method of *Wolfe and Silver* [1998], which treats multiple events simultaneously by normalizing and summing individual error surfaces, assuming that splitting observations do not exhibit back-azimuthal variations more complex than a single anisotropic layer with a vertical symmetry axis. The absence of significant back-azimuthal variations suggests that this assumption is satisfied for stations more than 20 km outside the shear zone [*Eaton and Hope*, 2003]; for a cluster of stations inside the shear zone we have performed further analyses (see below). Error contours were determined by assuming that the data follow an *F*-distribution. For each single-event error surface, the number of degrees of freedom was taken to be the minimum time between correlated events divided by the window length [*Yang et al.*, 1995].

[9] Average fast-axis directions (ϕ_S) vary in a systematic manner across the profile (Figure 1b). Stations at both ends of the profile are characterized by single-layer splitting behavior with ϕ_S of N55°E to N59°E, similar to geoelectric strike directions for lithospheric mantle periods as well as regional fast-axis orientations in the Slave craton north of the present study [*Bank et al.*, 2000]. Near the center of the profile, ϕ_S rotates to a minimum value of N35°E, similar to the geoelectric strike directions for crustal periods. This fine-scale variability in splitting behavior is also evident upon inspection of the filtered transverse-component seismograms for an individual event (Figure 2). Based on Fresnel-zone considerations, the short-scale length of these variations implies the presence of shallow (crustal) anisotropy. Given the dominant period for this event of ~4 s, for example, an anisotropic layer at 40 km depth is expected to influence surface observations to a distance range of between 20 km [*Alsina and Snieder*, 1995] and 50 km [*Rumpker and Ryberg*, 2000].

3. Two-Layer Seismic Inversion

[10] Seismic stations near the center of our profile exhibit significant back-azimuthal variations in apparent splitting parameters (Figure 3), suggesting an anisotropy structure more complex than a single anisotropic layer. Lateral changes in anisotropy, 3-D structure, a non-horizontal

[1]Auxiliary material is available at ftp://ftp.agu.org/apend/gl/2004GL020939.

fast-axis orientation, the presence of more than one anisotropic layer, or some combination of these factors can all give rise to such variability. Given an adequate distribution of events, it is sometimes possible to distinguish two-layer anisotropy from these other scenarios based on apparent splitting parameters [*Silver and Savage*, 1994]. For our study, the back-azimuthal distribution is insufficient to make such a determination; we are motivated, however, to explore the possibility of two layers based on the MT results.

[11] To estimate apparent two-layer anisotropy parameters we have applied the waveform inversion method of *Özalaybey and Savage* [1994] to our best quality split waveforms recorded by the cluster of four seismograph stations near the center of our profile. This inversion method is very similar to the multi-event averaging technique of *Wolfe and Silver* [1998], except that the effects of two-layer (rather than single-layer) splitting are modeled. Errors were estimated in the same way as for the single-layer inversion, except that the *F*-test was applied using four model parameters rather than two. Our results do not depend strongly on the specific subset of events considered (Table 1). Using all 5 events, the inversion yielded model parameters of 20° ± 5° and 66° ± 7° for the fast-axis directions of the shallow and deep layers, respectively, with corresponding splitting times of 0.8 ± 0.1 s and 0.6 ± 0.1 s. The pattern of apparent single-layer splitting parameters predicted by this model is in good agreement with the observed data (Figure 3).

4. Discussion

[12] The *S*-wave splitting results provide evidence that a deep, regional anisotropic layer with a fast direction of ~N60°E extends beneath the shear zone, and is overlain by a localized crustal anisotropic zone with a fast direction of ~N20°E. Although both the electric and seismic responses are sensing crustal deformation, the MT response appears to be more sensitive to features at greater distances from the shear zone. *Silver and Savage* [1994] and *Hartog and Schwartz* [2001] have reported two-layer seismic anisotropy structure for the San Andreas fault; in their models, however, the shallow anisotropic layer is closely aligned with the fault zone. In the case of the GSLsz the brittle upper crust has been removed, so the shallow anisotropy is manifested in rocks that were most likely deformed under mid-crustal conditions. We note that the shallow anisotropy direction is approximately parallel to the local strike of a conspicuous positive magnetic anomaly (Figure 1), the wavelength of which (30 km) precludes a mantle source [*Eaton and Hope*, 2003]. It is not necessary to invoke

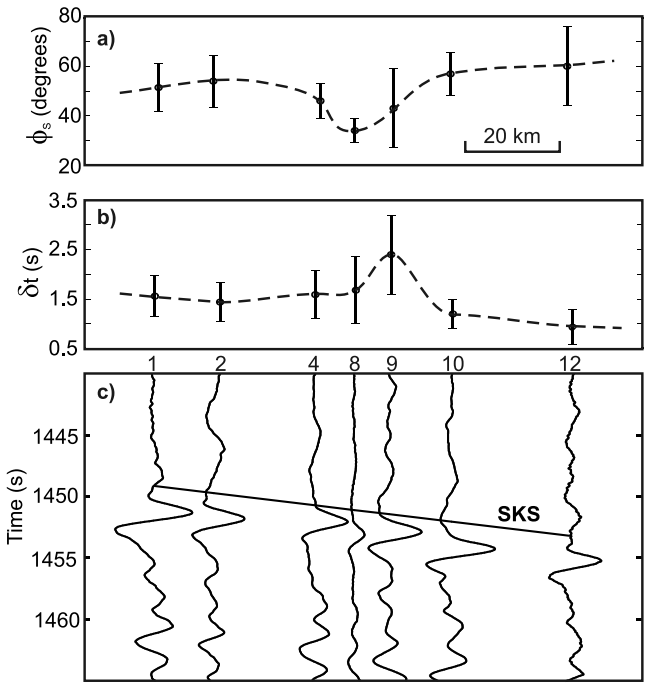

Figure 2. Splitting analysis for an M = 6.4 earthquake in the Celebes Sea on 1999/06/18. Parameters ϕ_S (a) and δt (b), as well as the transverse waveform (c), are anomalous within the shear zone.

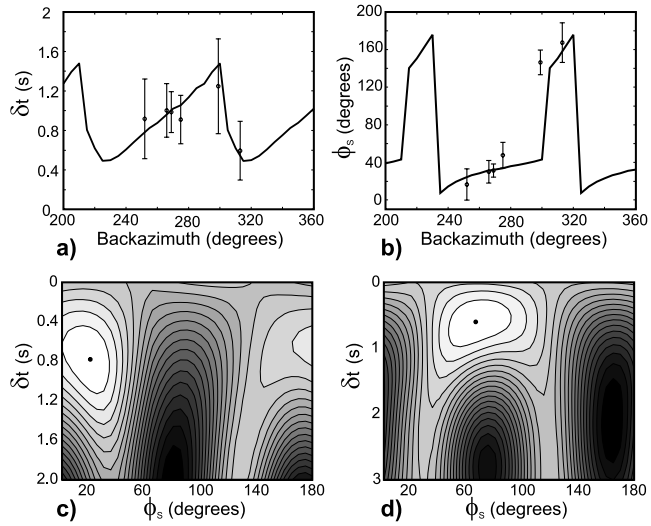

Figure 3. Two-layer splitting analysis for a cluster of 4 stations within the shear zone. Single-event splitting parameters (symbols) in (a) and (b) show azimuthal variations that are inconsistent with single-layer anisotropy. Two-parameter energy contour plots for shallow (c) and deep (d) layers are extracted from the total energy of the reconstructed transverse component trace, using a two-layer waveform inversion scheme [*Özalaybey and Savage*, 1994]. Contour interval is 5% of maximum energy difference. Solid curves in (a) and (b) show forward calculation of azimuthal variations, using the inversion results from (c) and (d).

Table 1. Results of Teleseismic Stacking Experiment Using the Two-Layer Inversion Method of *Özalaybey and Savage* [1994], for the Cluster Near Station 5

BAZ (degrees)	ϕ_{S1}[a] (degrees)	δt_1 (s)	ϕ_{S2} (degrees)	δt_2 (s)
253	−2 ± 6	0.6 ± 0.1	45 ± 6	0.7 ± 0.1
277	84 ± 15	0.3 ± 0.2	40 ± 10	0.9 ± 0.2
298	31 ± 3	1.1 ± 0.2	74 ± 13	0.3 ± 0.1
300	5 ± 7	0.6 ± 0.2	56 ± 4	1.2 ± 0.2
314	14 ±11	0.6 ± 0.1	55 ± 5	1.1 ± 0.3
253+314	13 ± 7	0.7 ±0.1	61 ± 5	0.7 ± 0.3
253+300+314	14 ± 5	0.7 ± 0.1	62 ± 4	0.9 ± 0.1
All	20 ± 5	0.8 ± 0.1	66 ± 7	0.6 ± 0.1

[a]Estimated splitting parameters are given with 95% confidence limits; subscripts 1 and 2 refer to shallow and deep layers, respectively.

crustal decoupling or different deformation mechanisms to explain the localized obliquity of these crustal fabrics with respect to mantle anisotropy and the N55°E regional strike of the shear zone; this relationship can be explained by a transpressive transfer zone, or late-stage shear deformation wrapping around a constriction [*Wu et al.*, 2002].

[13] Aside from localized crustal anisotropy within the GSLsz, we cannot determine the depth location of anisotropy based on *S*-wave splitting data alone. The strong similarity between the shear-wave fast-axis direction and the distinct MT strike direction (∼N60°E) of the lithospheric upper mantle suggests that both may be characteristic of the same depth interval. This scenario, our preferred interpretation, is consistent with inferred parallel seismic anisotropy and geoelectric strike observed elsewhere, such as in the mantle beneath northern Australia [*Simpson*, 2001]. Alternatively, if the seismic anisotropy is localized near the base of the lithosphere, as predicted by the absolute plate-motion anisotropy hypothesis of *Vinnik et al.* [1992], it implies that the seismic fast axis is slightly oblique to the corresponding N70°E geoelectric strike at this depth.

[14] Hydrogen diffusion along olivine *a*-axes [*Bahr and Simpson*, 2002] is consistent with parallel ϕ_S and ϕ_{MT}, since ϕ_S generally corresponds with the mean *a*-axis orientation for olivine in the upper mantle [*Savage*, 1999]. On the other hand, the model of *Ji et al.* [1996] predicts a clockwise rotation of ϕ_S relative to ϕ_{MT} for a dextral transform fault such as the GSLsz. The sense of obliquity can be regarded as equivalent to classical schistosité-cisaillement (*S*-*C*) fabrics [*Hanmer and Passchier*, 1991], in which ϕ_S and ϕ_{MT} approximately define *C*- and *S*-planes, respectively. Regardless of the depth location of seismic anisotropy, our results show either parallel orientations of *S*-wave fast axis and upper-mantle MT strike direction, or evidence for crustal distortion of the *S*-wave polarization direction that invalidates such a comparison. Although it brings into question its general applicability to mantle shear zones, the lack of obliquity does not falsify the hypothesis since *S*- and *C*-planes become parallel under conditions of high strain [*Hanmer and Passchier*, 1991].

5. Conclusions

[15] Approximately collocated magnetotelluric (MT) and teleseismic shear-wave splitting measurements were obtained across the Great Slave Lake shear zone in northern Canada to test the obliquity hypothesis of *Ji et al.* [1996]. Band-limited geoelectric strike vectors are oriented at N30°E, N60°E and N70°E for periods most sensitive to the crust, upper lithospheric mantle, and deep lithosphere/asthenosphere, respectively. *S*-wave splitting results are consistent with a deep, regional anisotropic layer with a fast direction of ∼N60°E, overlain by a crustal anisotropic zone with a fast direction of ∼N20°E, localized near the shear zone. Our data show how such comparisons may be useful for interpreting the depth location of seismic anisotropy, but do not provide evidence for systematic obliquity between seismic and electrical anisotropy in the upper mantle beneath the Great Slave Lake shear zone.

[16] **Acknowledgments.** The authors wish to acknowledge Phoenix Geophysics and Nick Grant for high quality MT data acquisition. Isa Asudeh, the staff of the GSC Yellowknife observatory and Stephane Rondenay are thanked for assistance with the teleseismic experiment. This work was supported by NSERC, Lithoprobe, the GSC and IRIS-PASSCAL.

References

Alsina, D., and R. Snieder (1995), Small-scale sublithospheric continental mantle deformation: Constraints from SKS splitting observations, *Geophys. J. Int.*, *123*, 431–448.

Bahr, K., and F. Simpson (2002), Electrical anisotropy below slow- and fast-moving plates: Paleoflow in the upper mantle?, *Science*, *295*, 1270–1272.

Bank, C. G., M. G. Bostock, R. M. Ellis, and J. F. Cassidy (2000), A reconnaissance teleseismic study of the upper mantle and transition zone beneath the Archean Slave craton in NW Canada, *Tectonophys.*, *319*, 151–166.

Eaton, D. W., and J. Hope (2003), Structure of the crust and upper mantle of the Great Slave Lake shear zone, northwestern Canada, from teleseismic analysis and gravity modeling, *Can. J. Earth Sci.*, *40*, 1203–1218.

Hanmer, S., and C. Passchier (1991), Shear-sense indicators: A review, Geol. Surv. Can., *Paper 90–17*, 72 pp., Geol. Surv. Can., Ottawa, Ontario.

Hanmer, S., S. Bowring, O. van Breemen, and R. Parrish (1992), Great Slave Lake shear zone, NW Canada: Mylonitic record of Early Proterozoic continental convergence, collision and indentation, *J. Struct. Geol.*, *14*, 757–773.

Hartog, R., and S. Y. Schwartz (2001), Depth-dependent mantle anisotropy beneath the San Andreas fault system: Apparent splitting parameters and waveforms, *J. Geophys. Res.*, *106*, 4155–4168.

Hoffman, P. F. (1987), Continental transform tectonics: Great Slave Lake shear zone (ca. 1.9 Ga), northwest Canada, *Geology*, *15*, 785–788.

Ji, S., S. Rondenay, M. Mareschal, and G. Senechal (1996), Obliquity between seismic and electrical anisotropies as a potential indicator of movement sense for ductile shear zones in the upper mantle, *Geology*, *24*, 1033–1036.

Jones, A. G. (1992), Electrical properties of the lower continental crust, in *Continental Lower Crust*, edited by D. Fountain et al., pp. 81–143, Elsevier Sci., New York.

Mareschal, M., R. Kellett, R. D. Kurtz, J. N. Ludden, S. Ji, and R. C. Bailey (1995), Archean cratonic roots, mantle shear zones and deep electrical anisotropy, *Nature*, *375*, 134–137.

McNeice, G., and A. G. Jones (2001), Multisite, multifrequency tensor decomposition of magnetotelluric data, *Geophysics*, *66*, 158–173.

Özalaybey, S., and M. K. Savage (1994), Double-layer anisotropy resolved from S phases, *Geophys. J. Int.*, *117*, 653–664.

Ross, G. M. (2002), Evolution of continental lithosphere in western Canada: A synthesis of lithoprobe studies in Alberta and beyond, *Can. J. Earth Sci.*, *39*, 413–437.

Rumpker, G., and T. Ryberg (2000), New "Fresnel-zone" estimates for shear-wave splitting observations from finite-difference modeling, *Geophys. Res. Lett.*, *27*, 2005–2008.

Savage, M. K. (1999), Seismic anisotropy and mantle deformation: What have we learned from shear wave splitting?, *Rev Geophys.*, *37*, 65–106.

Silver, P. G. (1996), Seismic anisotropy beneath the continents: Probing the depths of geology, *Annu. Rev. Earth Planet. Sci.*, *24*, 385–432.

Silver, P. G., and W. W. Chan (1991), Shear-wave splitting and subcontinental mantle deformation, *J. Geophys. Res.*, *96*, 16,429–16,454.

Silver, P. G., and M. K. Savage (1994), The interpretation of shear-wave splitting parameters in the presence of two anisotropic layers, *Geophys. J. Int.*, *119*, 949–963.

Simpson, F. (2001), Resistance to mantle flow inferred from the electromagnetic strike of the Australian upper mantle, *Nature*, *412*, 632–635.

Vinnik, L. P., L. I. Makeyeva, A. Milev, and A. Y. Usenko (1992), Global patterns of azimuthal anisotropy and deformations in the continental mantle, *Geophys. J. Internat.*, *111*, 433–447.

Wolfe, C. J., and P. G. Silver (1998), Seismic anisotropy of oceanic upper mantle: Shear wave splitting methodologies and observations, *J. Geophys. Res.*, *103*, 749–771.

Wu, X., I. J. Ferguson, and A. G. Jones (2002), Magnetotelluric response and geoelectric structure of Great Slave Lake shear zone, *Earth Planet. Sci. Lett.*, *96*, 35–50.

Yang, X., K. M. Fischer, and G. Abers (1995), Seismic anisotropy beneath the Shuagin Islands segment of the Aleutian-Alaska subduction zone, *J. Geophys. Res.*, *100*, 18,165–18,177.

D. W. Eaton, Department of Earth Sciences, University of Western Ontario, London, Ontario, Canada N6A 5B7.

I. J. Ferguson, Department of Geological Sciences, University of Manitoba, Winnipeg, Manitoba, Canada R3T 2N2.A.

G. Jones, School for Cosmic Physics, Dublin Institute for Advanced Studies, 5 Merrion Square, Dublin 2, Ireland.